Local Stability at Nozzles in Spherical Shells Subjected to Bending Moments and Axial Forces

S. Bantle
TOR Gesellschaft für technisch orientiertes Rechnen m.b.H., Zerzabelshofstr. 76, D-8500 Nürnberg 30, Germany
H. Calli, J. Jeschke
Kraftwerk Union AG, Berliner Str. 295-299, D-6050 Offenbach, Germany

Summary

The stability of spherical shells including nozzles and reinforced rounds has been investigated theoretically for the loading external force and overturning moment. Limit loads have been established for several geometries emphasizing the overturning moment.

1 Introduction

External forces or overturning moments acting on nozzles, or jet forces due to pipe rupture, may cause stability problems in the shells. Independent of their sign overturning moments always yield tension and compression membrane stress resultants in the shell, whereas the external forces must act inwards in relation to the shells surface to represent a stability problem. In case that the diameter of the nozzle loaded with forces or moments, or the extension of the load area of the jet force, is small enough compared with the shell diameter and wall thickness, local stability will govern, which does not influence the overall stability rather than the leaktightness.

References dealing with these problems, especially overturning moments acting on spherical caps reinforced with rounds, scarcely can be found in literature. Nevertheless these cases are relevant e. g. for the metal containment of pressurized light water reactors. Therefore the present paper deals with nozzles in a spherical shell, reinforced with rounds. The nozzles are loaded with external force or overturning moment, using the latter as an example.

2 Starting Point

To establish practical forces and moments for nozzles on the basis of the stability criterion and, after division by the safety, allowable ones, several approaches have been used. E. g. based upon /1/ for point forces on reinforced spherical caps without cut-outs a practical buckling load F_o can be obtained using:

$$F_o = \pi \, T \, D \, q \qquad (1)$$

with T = thickness of the base shell, D = load diameter, q = specific buckling load. By means of /2/ it is possible to calculate a practical buckling moment:

$$M_o = F_o \, D \, / \, 4 \qquad (2)$$

However, there are some uncertainties in this procedure: The test specimen did not include nozzles in the shell. Furthermore certain ratios of round diameter to round thickness have to be met. This results in possible uneconomical design. Moreover only elastic pretests are presented in /2/. No buckling tests for overturning moments were carried out. Therefore it was felt that the formula (2) may not be verified sufficiently.

3 Calculations and Results

To check formula (2), limit load analyses using the code STAGSC /3/ have been carried out, taking into account geometries which were designed according to the philosophy shown in /4/ (see Fig. 1 and Table 1).
The theory of moderate displacements as well as an elastic-plastic material law were applied (see Table 2). The load-deflection-curves obtained are shown in Fig. 2, including the limit load overturning moment M_{Tr}.

Two different structural behaviours have been found: For a ratio of round wall thickness to base shell wall thickness TR/T < 1.6 the load-deflection-curve continues to rise after first maximum under considerable increase in the deflections until the limit load is obtained (see Fig. 2, NW 290, NW 600, NW 940).
A similar behaviour was shown for external forces in /6/. This stiffening effect was no longer found for TR/T > 1.6. Thus the displacements have been accordingly smaller when the M_{Tr} have been found. The thickness and the length of the nozzles as well as the small differences in the yield stresses were not relevant for the different structural behaviours. Geometries with comparatively thick rounds (in our case TR/T > 1.6) show yielding in the base shell first. Thus there is neither a stress redistribution from the round into the base shell nor a resulting stiffening effect.
Relating the M_{Tr} to the governing geometry parameters TS, TR, DR, resp. (see Fig. 1), and maintaining R and T constantly, we obtain the dimensionless limit load overturning moments m_{Tr} (see Fig. 3).
The limit load analyses were accompanied by checks and additional investigations to control, whether there will be a bifurcation point or not, before the limit load is reached. To simplify matters axisymmetric calculations have been carried out taking as a basis the worst meridian, related to the membrane stress resultants, using the code KSHEL /5/ and the linear prebuckling theory.
In addition, for several load steps PA in the course of the STAGSC computation the bifurcation buckling loads have been evaluated. Again, the basis for the axisymmetric calculation has been the worst meridian related to the membrane stress resultants. This procedure is adequate to a non-linear prebuckling analysis. As an example Tab. 3 shows the result for NW 1310.

4 Conclusions

The limit load analyses shown have been carried out without initial imperfections. Once the overturning moment is applied, the axisymmetry of the geometry vanishes. Thus the influence of initial imperfections is assumed to be negligible. Therefore no additional knock-down factor has to be established to obtain allowable overturning moments from the M_{Tr}. Tab. 4 shows, as suspected, that the M_o calculated on the basis of eq. (2) are considerably too small. Taking into consideration that there are large displacements for some M_{Tr}, demanding a deformation limit for structural reasons, it is found that eq. (2) yields results which are at least $\pi/2$ too small.
Relating to the external forces acting upon nozzles, similar investigations have been possible. Only a small increase compared with the results obtained with eq. (1) appears in outlines.

5 References

/1/ WELLINGER, K., LORENZ, K., "Senkrechte ring- und punktförmige Krafteinleitung in Kugelschalen", Technische Mitteilungen aus dem Dampfkessel-, Behälter- und Rohrleitungsbau, GKW-Verband, Düsseldorf (August 1958) (I).

/2/ WELLINGER, K., LORENZ, K., "Zwischenbericht über Momenteinleitung in Kugelschalen", Technische Mitteilung aus dem Dampfkessel-, Behälter- und Rohrleitungsbau, GKW-Verband, Düsseldorf (August 1958) (II).

/3/ ALMROTH, B.O, BROGAN, F.A., STANLEY, G.M., "Structural Analysis of General Shells, User Instructions for STAGSC", Lockheed Palo Alto Research Laboratory, Palo Alto, California (December, 1975).

/4/ ANDERSEN, A., BANTLE, S., "Optimization of Containment Nozzles", paper J 6/8, presented at 5th Intl. Conf. on Structural Mechanics in Reactor Technology, Berlin, West Germany, (August 1979).

/5/ KALNINS, A., "Analysis of Shells of Revolution Subjected to Symmetrical and Nonsymmetrical Loads", "Journal of Applied Mechanics" 31, 467-476 (1964).

/6/ PENNING, F.A., THURSTON, G.A., "The Stability of Shallow Spherical Shells under Concentrated Load", NASA CR-265, National Aeronautics and Space Administration, Washington, D.C. (1965).

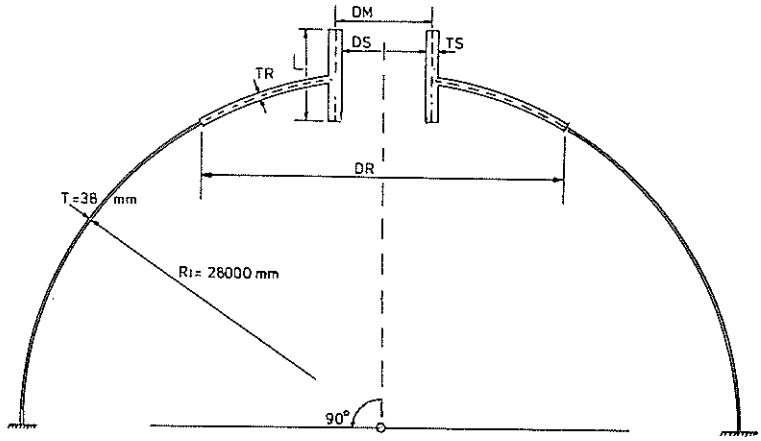

Fig. 1: Investigated Geometries

Tab. 1

Investigated Geometries						
NW	DS	TS	TR	L	DR	DM
	mm	mm	mm	mm	mm	mm
290	290	60	60	380	1644	350
600	600	70	60	390	1286	670
940	945	80	60	420	2500	1025
1310	1310	80	80	420	3000	1390
1450	1450	85	80	520	3000	1535
3000	3207	110	80	1720	5027	3317
4000	4000	130	80	770	6500	4130

Tab. 3

PA from STAGSC	Theoretical Buckling Moment (Nonlinear) M_{nl} = PRMLT · PA · M										
	NW 1310 (M = 210 kNm)										
	circumferential wave numbers N										
	0	1	2	3	4	5	6	7	8	9	10
8.2	12.6	12.37	14.2	17.19	19.67	23.08	-37.66	-34.4	-34.48	-36.4	-39.4
17.8	5.29	5.214	5.962	7.107	8.055	9.371	-13.57	-12.61	-12.75	-13.56	-14.75
20.775	4.388	4.297	4.939	5.784	6.3	-9.133	-7.629	-7.627	-7.463	-7.986	-8.777

Tab. 2

Yield Point Values			
NW	Stress N/mm²		
	shell	rond	nozzle
290	370	330	320
600	370	330	330
940	370	330	310
1310	370	330	310
1450	370	330	310
3000	370	330	310
4000	370	330	310

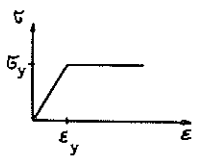

E = 211000 N/mm²

Tab. 4

Comparison of Limit Load Overturning Moments		
NW	M_o kNm	$\frac{M_{Tr}}{M_o}$
290	522	> 11,6
600	286	13,7
940	1583	3,77
1310	2243	1,95
1450	2243	2,04
3000	8635	1,76
4000	15456	1,67

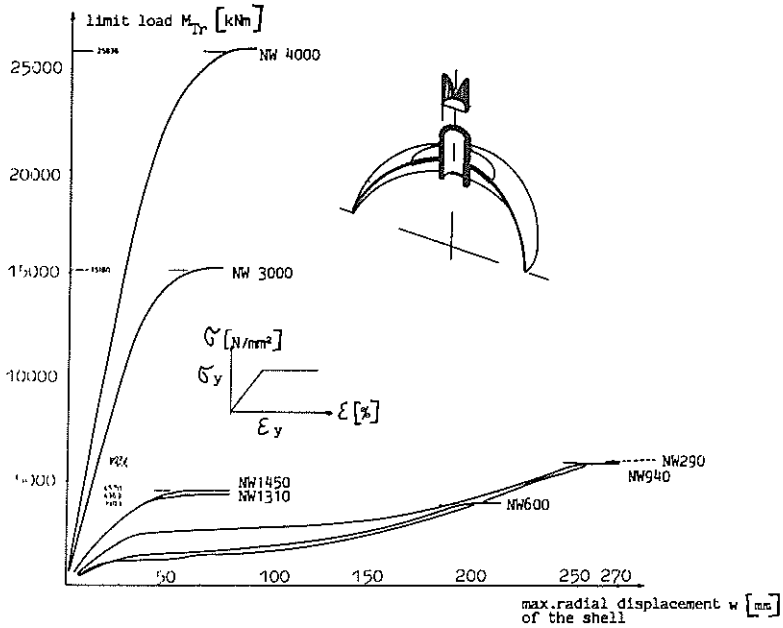

Fig. 2: Load-Deflection Diagram and Limit Load Overturning Moments

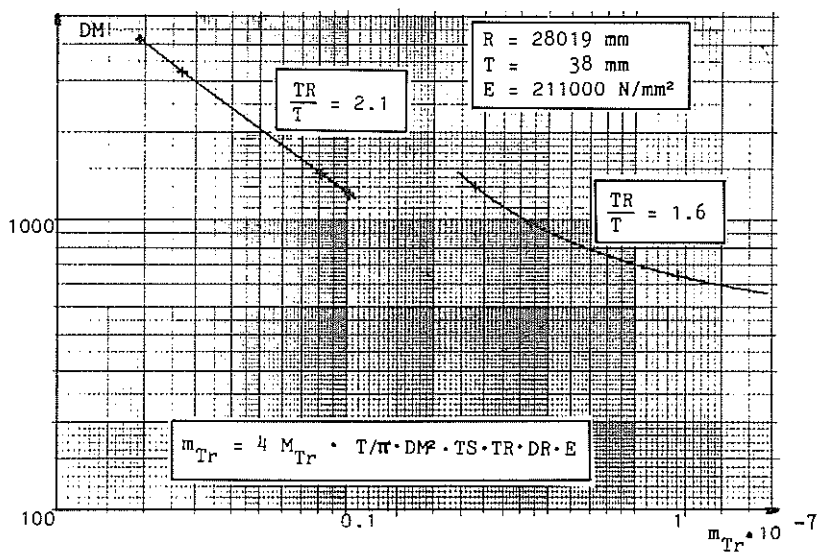

Fig. 3: Dimensionless Limit Load Overturning Moments